American Journal of Pathology, Vol. 167, No. 1, July 2005

Neurobiology

Age-Related Loss of Synaptophysin Immunoreactive Presynaptic Boutons within the Hippocampus of APP751^{SL}, PS1^{M146L}, and APP751^{SL}/PS1^{M146L} Transgenic Mice

Bart P.F. Rutten,*† Nicolien M. Van der Kolk,*† Stephanie Schafer,†‡ Marc A.M.J. van Zandvoort,§ Thomas A. Bayer,†‡ Harry W.M. Steinbusch,*† and Christoph Schmitz*†

From the Department of Psychiatry and Neuropsychology, Division of Cellular Neuroscience, Maastricht University, Maastricht, The Netherlands; the European Graduate School of Neuroscience,† EURON, Maastricht, The Netherlands; the Department of Psychiatry,‡ Division of Neurobiology, University of the Saarland Medical Center, Homburg/Saar, Germany; and the Department of Biophysics,§ Maastricht University, Maastricht, The Netherlands*

Neuron and synapse loss are important features of the neuropathology of Alzheimer's disease (AD). Recently, we observed substantial age-related hippocampal neuron loss in APP751^{SL}/PS1^{M146L} transgenic mice but not in PS1^{M146L} mice. Here, we investigated APP751^{SL} mice, PS1^{M146L} mice, and APP751^{SL}/PS1^{M146L} mice for age-related alterations in synaptic integrity within hippocampal stratum moleculare of the dentate gyrus (SM), stratum lucidum of area CA3 (SL), and stratum radiatum of area CA1–2 (SR) by analyzing densities and numbers of synaptophysin-immunoreactive presynaptic boutons (SIPBs). Wild-type mice, APP751^{SL} mice and PS1^{M146L} mice showed similar amounts of age-related SIPB loss within SM, and no SIPB loss within SL. Both APP751^{SL} mice and PS1^{M146L} mice showed age-related SIPB loss within SR. Importantly, APP751^{SL}/PS1^{M146L} mice displayed the severest age-related SIPB loss within SM, SL, and SR, even in regions free of extracellular Aβ deposits. Together, these mouse models offer a unique framework to study the impact of several molecular and cellular events caused by mutant APP and/or mutant PS1 on age-related alterations in synaptic integrity. The observation of age-related SIPB loss within SR of PS1^{M146L} mice supports a role of mutant PS1 in neurodegeneration apart from its contribution to alterations in Aβ generation. *(Am J Pathol 2005, 167:161–173)*

Alzheimer's disease (AD) is a progressive neurodegenerative disorder comprising cognitive and memory deterioration, progressive impairment of activities of daily living, and several neuropsychiatric symptoms.[1] The neuropathology of AD is characterized by disturbances in neural circuits, such as loss of neurons and synapses, and by protein aggregations of β-amyloid and hyperphosphorylated tau.[2–4] Accumulating evidence has indicated a crucial role for failure and loss of synapses in AD pathophysiology.[2,4,5–7] Postmortem morphological studies on AD neuropathology have demonstrated significantly reduced synaptic connectivity in brain regions such as the neocortex and hippocampus.[3,6,7] Reductions in synaptic densities showed a strong correlation with cognitive decline in AD.[5] However, the reasons for the reduced connectivity in AD remain poorly understood.[8] According to the "β-amyloid (Aβ) hypothesis of AD," Aβ accumulation is the primary driving force in AD pathogenesis. This hypothesis is supported by the fact that mutations in the amyloid precursor protein (APP) and in presenilin (PS) 1 and PS2, causing early-onset cases of AD, modify APP processing and result in enhanced generation of Aβ.[4] We have developed a transgenic mouse model of AD expressing human mutant APP751 (carrying the Swedish and London mutations KM670/671NL and

Supported by the European Community (grants QLK6-CT-2000-60042, QLK6-GH-00-60042-07, and QLK6-GH-00-60042-15), Alzheimer Forschung Initiative e.V., Fritz Thyssen Foundation, and Internationale Stichting Alzheimer Onderzoek. The BioRad TPLSM was obtained by grant 902-16-276 from the Medical Section of the Dutch Scientific Organization (NWO).

Accepted for publication March 24, 2005.

Address reprint requests to Christoph Schmitz, M.D., Department of Psychiatry and Neuropsychology, Division Cellular Neuroscience, Maastricht University, P.O. Box 616, 6200 MD, Maastricht, The Netherlands. E-mail: c.schmitz@np.unimaas.nl.

V717I, Thy1 promoter; APP751^{SL} mice), human mutant presenilin-1 (PS1 M146L, HMG promoter; PS1^{M146L} mice) or both human mutant APP751 and human mutant presenilin-1 (APP751^{SL}/PS1^{M146L} mice) in neurons[9–12] (see also Refs. [8] and [13]). Similar to what happens in human AD, the amount of extracellular Aβ deposits as well as the level of reactive astrogliosis increase as these APP751^{SL} mice and APP751^{SL}/PS1^{M146L} mice age.[9–12] Furthermore, the APP751^{SL}/PS1^{M146L} mice show substantial age-related loss of hippocampal pyramidal cells.[12] Importantly, the amount of neuron loss exceeded the amount of Aβ deposits and associated reactive astrogliosis in these mice, indicating that the observed neuron loss was at least in part independent of Aβ deposits.[12] Given the popular belief that extracellular Aβ deposits are the cause of neuronal degeneration in AD,[4] these findings have prompted modification of the original "amyloid cascade" hypothesis for AD.[13,14]

It was the aim of the present study to test the hypothesis that these APP751^{SL} mice, PS1^{M146L} mice, and APP751^{SL}/PS1^{M146L} mice show region-specific, age-related alterations in synaptic integrity within the hippocampus, with region-specific differences among the investigated genotypes. Another aim was to determine to what extent these alterations in synaptic integrity were due to Aβ deposits within the hippocampus and to hippocampal neuron loss. The investigations were carried out by two-photon laser scanning microscopy, computerized image analysis and design-based stereology, focusing on densities and numbers of synaptophysin-immunoreactive presynaptic boutons (SIPBs). Analysis of SIPBs is a well-established approach for investigating alterations in synaptic integrity *in vivo* both in our[15,16] and in many other laboratories.[17–21]

Materials and Methods

Animals

The following groups of either 4.5-month-old (M4.5) or 17-month-old (M17) female mice were examined in the present study: wild-type control mice (C57Bl6 background; M4.5, $n = 6$; M17, $n = 6$), APP751^{SL} mice (transgenic mice expressing human mutant APP751 carrying the Swedish and London mutations KM670/671NL and V717I; Thy1 promoter; C57Bl6 [87.5%] $\times$ CBA [12.5%] background; M4.5, $n = 6$; M17, $n = 3$), PS1^{M146L} mice (transgenic mice expressing human mutant presenilin-1 [PS1 M146L]; HMG promoter; back-crossed on a C57Bl6 background for more than six generations;; M4.5: $n = 6$; M17: $n = 6$) and APP751^{SL}/PS1^{M146L} mice (APP/PS1 double-transgenic mice carrying the aforementioned APP and PS1 mutations; M4.5, $n = 6$; M17, $n = 6$). All mice were generated at the SanofiAventis Centre de Recherche de Paris (Vitry sur Seine, France) (for details, see Refs. [9–12]). The APP751^{SL}/PS1^{M146L} mice were generated by crossing homozygous PS1 mice to hemizygous APP751^{SL} mice. In the present study, hemizygous PS1^{M146L} littermates were used. All experiments were performed in accordance with the German animal protection law.

Tissue Processing

Mice were anesthetized with chloral hydrate and sacrificed by intracardial perfusion fixation with tyrode followed by fixative containing 4% paraformaldehyde, 15% picric acid and 0.05% glutaraldehyde in phosphate buffer (for details, see [12]). Brains were removed rapidly, halved in the mediosagittal line, and postfixed for 2 hours at 4°C in the fixative, omitting the glutaraldehyde. Brain tissue was then cryoprotected by immersion in 30% sucrose in Tris-buffered saline at 4°C overnight. Afterward, brains were quickly frozen and stored at −80°C until further processing. The right hemispheres were cut into entire series of 30-μm-thick frontal sections on a cryostat (Leica CM 3050; Leica, Nussloch, Germany). Afterward, these series were divided into 10 subseries of every 10th section each. The hippocampus was found on five to eight sections per subseries, depending on the individual rostrocaudal extension of the hippocampus. Four subseries of sections per animal (from the wild-type control mice, the PS1^{M146L} mice, and the APP751^{SL}/PS1^{M146L} mice but not from the APP751^{SL} mice) were used in a former study[12] to investigate age-related alterations in neuron numbers, the amount of Aβ deposits, apoptotic cell death, and microglia activation within the hippocampus. The left hemispheres were not used for the present study.

Investigation of Alterations in SIPB Morphology Due to Aβ Deposits

To investigate normal SIPB morphology and its alterations due to Aβ deposits, one subseries of sections per animal was used for immunohistochemical detection of both synaptophysin and β-amyloid (monoclonal mouse anti-synaptophysin antibody, 1:2000; Chemicon, Temecula, CA; rabbit anti-730 antibody detecting β-amyloid and P3,[22] 1:5000; generous gift from Dr. G. Multhaup). Briefly, fluorescent immunohistochemistry was carried out in a free-floating manner using standard protocols. Sections were incubated overnight at 4°C after rinsing with Tris-buffered saline (TBS) and TBS with Triton-X 100 and blocking of unspecific staining with 10% fetal calf serum and 4% nonfat-dry-milk in TBS. On the following day, the sections were rinsed and incubated with secondary antibodies for 1.5 hours at room temperature. Donkey anti-mouse IgG Alexa Fluor 488 antibody (1:100; Molecular Probes, Eugene, OR) and donkey anti-rabbit IgG Alexa Fluor 594 antibody (1:100; Molecular Probes), were used as secondary antibodies. Sections were mounted on gelatinized glass slides, dried, and coverslipped using 80% glycerol in PBS.

Sections were analyzed with standard fluorescence microscopy and two-photon laser scanning microscopy (TPLSM). TPLSM was performed as previously described[23] using a microscope objective (60×; water dipping; numerical aperture [NA] = 1.0) connected to an upright Nikon E600FN microscope (Nikon Corporation,

Tokyo, Japan). If needed, further magnification was achieved by optical zoom in the scan head. To remove noise, each image was filtered applying the Kalman filtering procedure on three subsequent images during experiments. The fluorescent secondary antibody Alexa 488 was mainly visible in the green channel, whereas Alexa 594 was only visible in the red channel, and the obtained images (coded green and red, respectively) were combined into single images if warranted.

Analysis of SIPB Densities

To analyze SIPB densities in various hippocampal subregions, one subseries of sections per animal was used for immunohistochemical detection of synaptophysin (monoclonal mouse anti-synaptophysin antibody; 1:2000; Chemicon; avidin-biotin immunoperoxidase labeling) (Figure 1, A to D). The M.O.M. immunodetection kit (Vector Laboratories, Peterborough, UK) was used according to the manufacturer's protocol to minimize background labeling and labeling of intraparenchymal IgG molecules. Control experiments comprised incubations without primary antibody and incubations without use of the M.O.M. immunodetection kit (Vector). All incubations were performed in a free-floating manner under exactly identical conditions. After labeling procedures, sections were mounted on gelatinized glass slides, dehydrated, coverslipped, and coded. The code was not broken until all analyses were completed.

SIPB densities were analyzed as previously described[15,16] within three subregions of the hippocampus: stratum moleculare of the dentate gyrus (SM), stratum lucidum of area CA3 (SL), and stratum radiatum of area CA1–2 (SR) (Figure 1E). Three randomly chosen areas per section were evaluated within SM and SR each, and two randomly chosen areas within SL (Figure 1E). Three high-power photomicrographs were taken from each evaluated area at approximately 2 μm below the upper surface of the sections (ie, when the SIPBs were clearly in focus) with a digital camera (F-view; Olympus, Tokyo, Japan) attached to an Olympus AX-70 microscope (100× oil objective; Olympus UplanApo, NA = 1.35). This procedure resulted in 45 to 72 photomicrographs for SM and SR each per animal (3 photomicrographs × 3 areas × [5 to 8] sections), and in 30 to 48 photomicrographs for SL per animal (2 photomicrographs × 3 areas × [5 to 8] sections) (Figure 1, F to H). In case of the APP751^{SL} mice and the APP751^{SL}/PS1^{M146L} mice, photomicrographs were exclusively taken at regions free of Aβ deposits and Aβ aggregation-related disturbances in normal SIPB morphology. Aβ deposits were clearly recognizable as round/oval structures not immunoreactive for synaptophysin and surrounded by multiple enlarged SIPBs and disturbed neuropil (Figure 1I). SIPBs were detected by image analysis using AnalySIS-pro software (Soft Imaging System, Münster, Germany), slightly modified for detection of grayscale punctae as previously described.[16] All settings were kept identical for all analyses. Shading error correction was performed before measurements were done to correct for irregularities in illumination of the microscopic fields. Furthermore, background levels were equalized. From these data, mean particle densities per square micrometer were calculated.

To enable the elimination of noise signal and to differentiate between possible artifacts and specific SIPBs, the normal size of SIPB was evaluated separately for SM, SL, and SR in a pilot experiment. For doing so, the area occupied by individual particles with a morphological appearance of SIPBs was measured separately within SM, SL, and SR in three wild-type mice using the AnalySIS-pro software (Soft Imaging System). A total of 400 particles was measured per hippocampal subregion. SIPB areas were, on average, 0.33 ± 0.12 μm^2 (mean ± SD) in SM, 1.02 ± 0.38 μm^2 in SL, and 0.36 ± 0.13 μm^2 in SR. The different SIPB size can be seen in Figure 1, F to H. A region-specific range of mean ± (2 × SD) was considered as normal SIPB size, and these settings were kept identical for all analyses. Size measurements of all SIPBs investigated in the present study indicated no differences in average SIPB size between the various groups of mice. Additional pilot studies (not described here) indicated that average SIPB size was independent from the plane of section (ie, identical results were obtained on frontal, sagittal, and horizontal sections of mouse brains).

Measuring Volumes of SM, SL, and SR

Volumes of SM, SL and SR were evaluated on the sections immunohistochemically processed for synaptophysin detection with avidin-biotin immunoperoxidase labeling with the aid of another subseries of sections per animal stained with cresyl-violet (Nissl) staining (0.01%) as previously described.[12,16] Briefly, the Nissl-stained sections were laid onto the corresponding adjacent sections processed with immunohistochemistry and were exactly aligned. Then SM, SL, and SR were delineated according to the literature[24] (Figure 1K). Delineation was carried out with a stereology workstation and StereoInvestigator software (MicroBrightField, Williston, VT) as previously described.[16] For doing so, the Nissl-stained sections were brought into focus. After delineation, these sections were removed; the sections processed with immunohistochemistry were brought into focus; and the boundaries of SM, SL, and SR were verified. Volumes of SM, SL, and SR were calculated with Cavalieri's principle[25,26] from the projection area measurements and the average actual section thickness after histological processing. The latter was measured with the electronic microcator of the stereology software and a 40× oil objective (Olympus UplanApo; NA = 1.00) as described previously.[26]

Calculation of SIPB Numbers

Hippocampal subregion-specific SIPB numbers were calculated by multiplying the individual SIPB density data with the corresponding volume data. Note that these SIPB numbers were not unbiased because SIPB densities were analyzed in one focal plane and thus in two dimensions instead of in three dimensions.[26] Thus, the

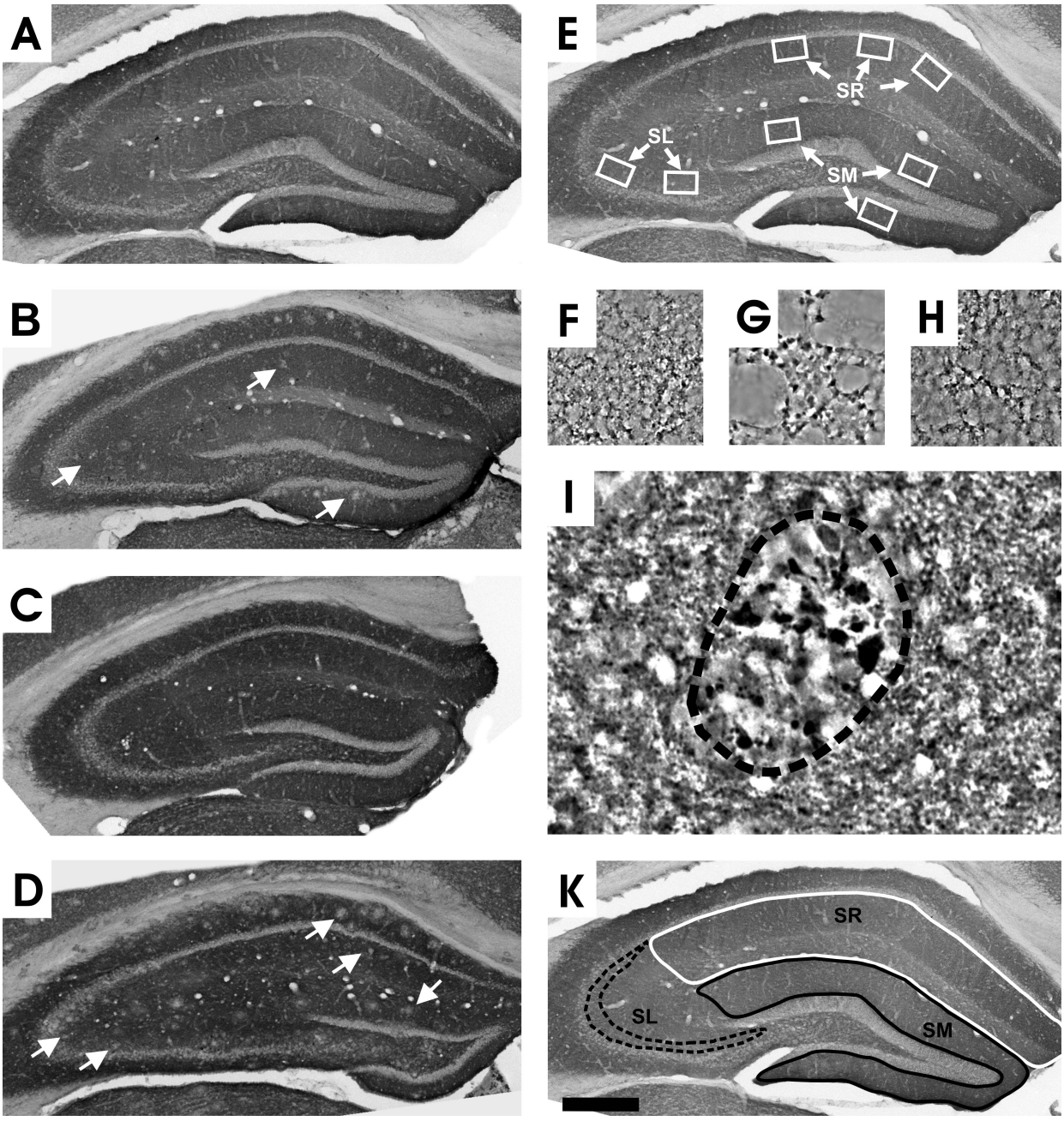

Figure 1. Representative photomicrographs of frontal sections through the hippocampus of a 17-month-old wild-type control mouse (**A**, **E** to **H**, and **K**), a 17-month-old APP751^{SL} mouse (**B**), a 17-month-old PS1^{M146L} mouse, and a 17-month-old APP751^{SL}/PS1^{M146L} mouse (**D** and **I**), showing immunoreactivity for synaptophysin. Aβ deposits within the hippocampus of the APP751^{SL} mouse and the APP751^{SL}/PS1^{M146L} mouse are indicated by **arrows** in **B** and **D**, respectively. The small squares in **E** represent the areas where the high-power photomicrographs for quantitative SIPB analysis were taken within SM, SL, and SR. Corresponding high-power photomicrographs depict larger SIPBs within SL (**G**) than within SM (**F**) and SR (**H**). Aβ deposits were clearly recognizable as round/oval structures not immunoreactive for synaptophysin and surrounded by multiple enlarged SIPBs and disturbed neuropil (**I**). The dotted line in **I** indicates the delineation of Aβ deposits as performed for the analysis of SIPB densities in regions free of Aβ deposits and Aβ aggregation-related disturbances in normal SIPB morphology. In **K**, the projection areas of SM, SL, and SR are shown. Scale bar = 250 μm in **A** to **E** and **K**, 20 μm in **F** to **H**, and 10 μm in **I**.

calculations did not take the dimensions of the investigated parameters (ie, 1/μm^2 [SIPB density] and mm^3 [volume]) into account. Importantly, this did not affect the results of the present study because for all groups of mice, similar distribution plots were obtained for individual SIPB size (not shown), and the average SIPB size was independent from the plane of section. Calculating unbiased total numbers of SIPBs was not the aim of the present study.

Calculation of Corrected SIPB Numbers

For the analysis of the APP751^{SL} mice and the APP751^{SL}/PS1^{M146L} mice the calculation of SIPB numbers resulted

in theoretical numbers assuming that Aβ deposits did not influence normal SIPB morphology (because SIPB densities were exclusively measured at regions free of Aβ deposits and Aβ aggregation-related disturbances in normal SIPB morphology as explained above). To take the impact of Aβ deposits on SIPB numbers into account, the percent volumes of SM, SL, and SR occupied by Aβ deposits and Aβ aggregation-related disturbances in normal SIPB morphology (as depicted in Figure 1I) were analyzed with point-counting methods[26,27] on the sections immunohistochemically processed for synaptophysin detection with avidin-biotin immunoperoxidase labeling. Point counting was performed on the stereology workstation with the 40× oil objective and a distance of 50 μm between the points in mutually orthogonal directions X and Y for SM and SR (and 20 μm for SL, respectively). Corrected SIPB numbers for the APP751^{SL} mice and the APP751^{SL}/PS1^{M146L} mice were calculated by subtracting the volume occupied by Aβ deposits and Aβ aggregation-related disturbances in normal SIPB morphology from the total volume of the investigated hippocampal subregions and by multiplying this value with the mean SIPB density found within the corresponding hippocampal subregion. Thus, corrected SIPB numbers for the APP751^{SL} mice and the APP751^{SL}/PS1^{M146L} mice were smaller than the corresponding uncorrected SIPB numbers. For the wild-type control mice and the PS1^{M146L} mice, the corresponding uncorrected SIPB numbers could serve as corrected SIPB numbers as well. This was due to the fact that these mice did not develop Aβ deposits.

Statistical Analysis

For each group of mice mean and SEM were calculated for all investigated variables (hippocampal subregion-specific SIPB density, volume of the subregion, SIPB number, and corrected SIPB number if applicable). Comparisons between the groups were performed separately for SM, SL, and SR with two-way analysis of variance (two-way ANOVA; four genotypes and two age groups per genotype) followed by Bonferroni posttests to compare replicate means focusing on age-related effects. Statistical significance was established at $P < 0.05$. All calculations were performed using GraphPad Prism (Version 4.00 for Windows; GraphPad Software, San Diego, CA).

Photography

Pictures shown in Figure 1, A to E and K, were generated with the stereology workstation using the Virtual Slice tool of the StereoInvestigator software, which automatically created high-resolution seamless image montages composed of approximately 100 individual fields-of-view visualized at high resolution. Photomicrographs shown in Figure 1, F to I, were taken with the Olympus AX-70 microscope. Pictures shown in Figures 2 and 3 were acquired using TPLSM. Image stacks were reconstructed into three-dimensional images followed by colocalization analysis with Imaris software (Bitplane, Zurich, Switzerland). Final figures were constructed using Corel Draw Version 11.0 (Corel, Ottawa, Canada) and Adobe Photoshop Version 7.0 (Adobe, San Jose, CA). Only minor adjustments of contrast and brightness were made, which in no case altered the appearance of the original materials.

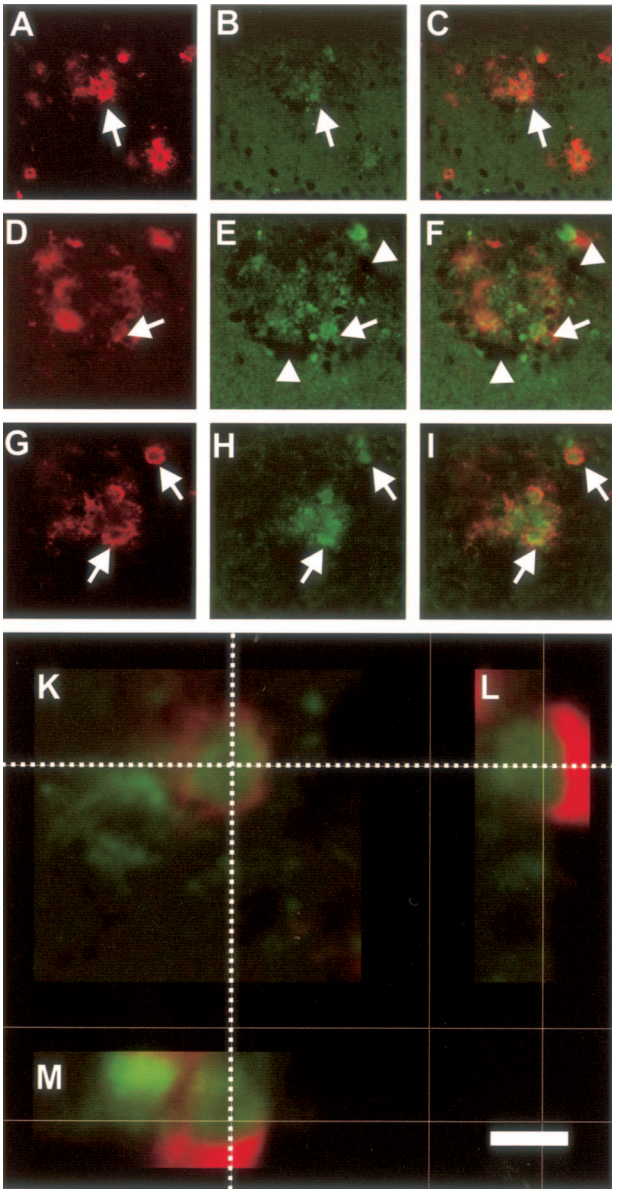

Figure 2. Representative high-power photomicrographs obtained by TPLSM, showing alterations in synaptic integrity caused by Aβ deposits within hippocampal subregion SR of a 17-month-old APP751^{SL}/PS1^{M146L} mouse. Aβ immunoreactivity is shown in red in **A**, **D**, and **G**; synaptophysin immunoreactivity at the corresponding locations and focal planes in green in **B**, **E**, and **H**; and merged pictures in **C**, **F**, and **I**. Note the disturbed SIPB morphology within and in the near vicinity of the Aβ deposits (**arrows**). The SIPB-free regions around the Aβ deposits (**arrowheads** in **E** and **F**) are most probably caused by astrocytes surrounding the Aβ deposits. Interestingly, several enlarged SIPBs were entirely surrounded by β-amyloid (**arrows** in **I**). In **K** to **M**, a three-dimensional reconstruction of a representative image stack acquired with TPLSM is shown, displaying synaptophysin (green) and Aβ (red) immunoreactivity within SR of a 17-month-old APP751^{SL}/PS1^{M146L} mouse. The **dotted lines** in **K** represent the position within the X-Y view at which the Y-Z view (**L**) and the X-Z view (**M**) were generated. The depicted enlarged synaptophysin-immunoreactive presynaptic bouton is surrounded by a rim of Aβ immunoreactivity. Scale bar = 100 μm in **A** to **C**, 50 μm in **D** to **I**, and 5 μm in **K** to **M**.

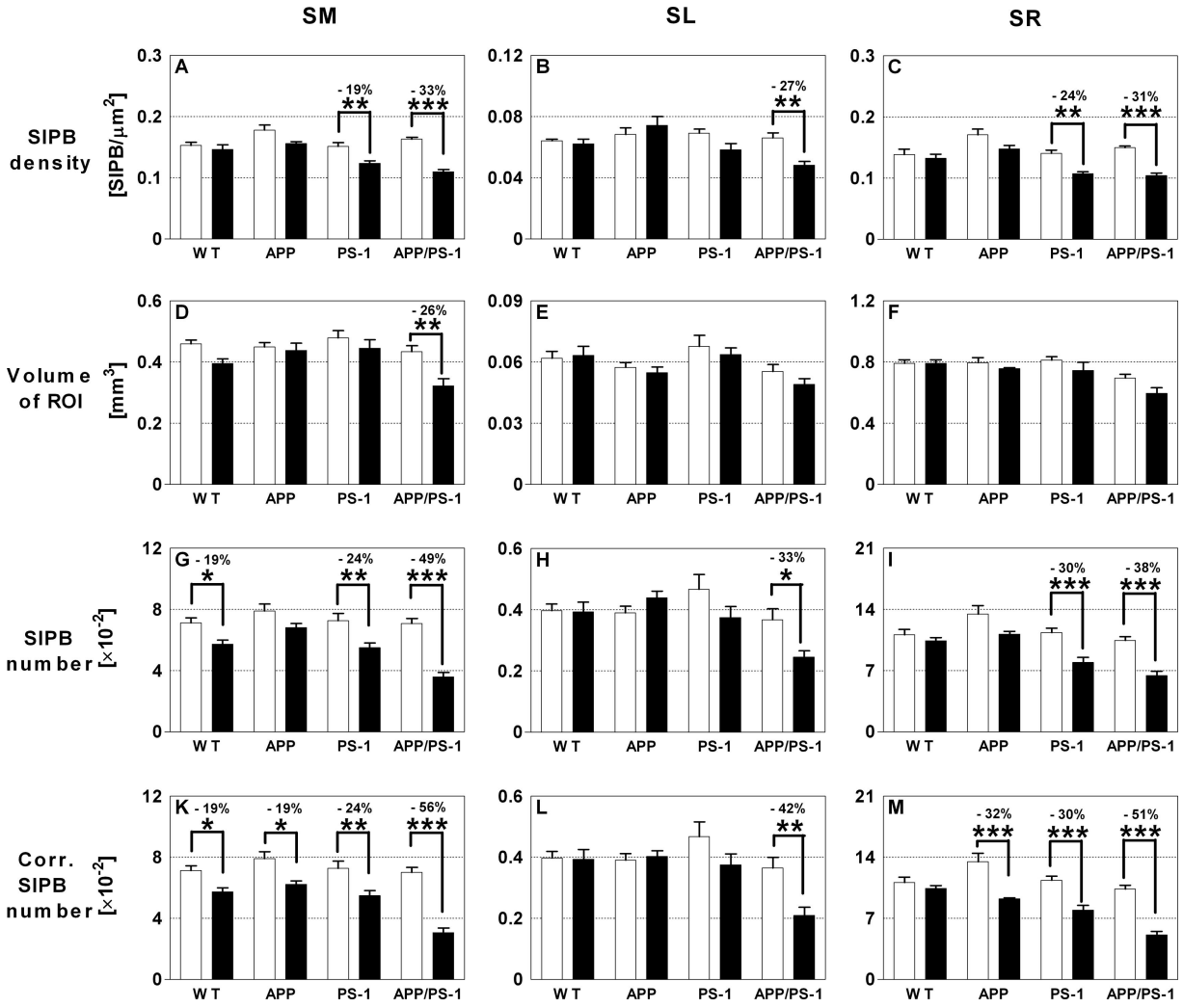

Figure 3. Results of the quantitative investigations in the hippocampus. Analysis of hippocampal SM (**A**, **D**, **G**, and **K**), SL (**B**, **E**, **H**, and **L**), and SL (**C**, **F**, **I**, **M**) of wild-type control mice (WT), APP751^{SL} mice (APP), PS1^{M146L} mice (PS1), and APP751^{SL}/PS1^{M146L} mice (APP/PS1) for age-related alterations in SIPB densities within regions free of Aβ deposits and Aβ aggregation-related disturbances in normal SIPB morphology (**A** to **C**); volumes of SM, SL, and SR (**D** to **F**); SIPB numbers within regions free of Aβ deposits and Aβ aggregation-related disturbances in normal SIPB morphology (**G** to **I**); and corrected SIPB numbers considering the amount of Aβ deposits within SM, SL, and SR (**K** to **M**). Results of 4.5-month-old mice (M4.5) are represented by **open bars**; those of 17-month-old mice (M17) by **closed bars**. Data are given as mean and SEM. Comparisons between the groups were performed separately for SM, SL, and SR with two-way ANOVA (P values summarized in Table 1) followed by Bonferroni posttests to compare replicate means focusing on age-related effects (P values provided as $^{*}P < 0.05$, $^{**}P < 0.01$, or $^{***}P < 0.001$ in **A**, **B**, **C**, **D**, **G**, **H**, **I**, **K**, **L**, and **M**). Significant differences in mean data are indicated (M17 versus M4.5) above each graph. ROI, region of interest; Corr., corrected. SIPB numbers were calculated by multiplying the individual SIPB density data with the corresponding volume data not considering the dimensions (see Materials and Methods for details).

Results

Alterations in SIPB Morphology Due to Aβ Deposits

Aβ deposits within the hippocampus were detected in APP751^{SL} mice at M17 and in APP751^{SL}/PS1^{M146L} mice at M4.5 and M17. No synaptophysin immunoreactivity was observed within the core of the Aβ deposits. Regions directly adjacent and surrounding the Aβ deposits showed substantial alterations in synaptophysin immunoreactivity. Specifically, considerably enlarged SIPBs were detected (up to 8 μm in diameter) close to the Aβ deposits (Figure 2). Three-dimensional reconstruction of TPLSM image stacks showed that some of these enlarged SIPBs were surrounded by Aβ (Figure 2).

SIPB Densities

Two-way ANOVA showed statistically significant age- and genotype-related differences in mean SIPB densities within SM, SL, and SR (all P values of two-way ANOVA are summarized in Table 1). Bonferroni posttests showed a significant age-related decline in mean SIPB densities within SM for the PS1^{M146L} mice (on average, −19%) and the APP751^{SL}/PS1^{M146L} mice (−33%), within SL only for the APP751^{SL}/PS1^{M146L} mice (−27%), and within SR for the PS1^{M146L} mice (−24%) and the APP751^{SL}/PS1^{M146L}

Table 1. Results of Two-Way ANOVA

		SM	SL	SR
SIPB density	Age	<0.001	0.009	0.001
	Genotype	<0.001	0.014	0.001
	Interaction	0.001	0.004	0.015
Volume of the subregion	Age	0.001	0.002	<0.001
	Genotype	<0.001	0.290	0.036
	Interaction	0.114	0.755	0.440
SIPB no.	Age	<0.001	0.004	<0.001
	Genotype	<0.001	0.077	<0.001
	Interaction	0.018	0.059	0.024
Corrected SIPB no.	Age	<0.001	0.001	<0.001
	Genotype	<0.001	0.016	<0.001
	Interaction	0.004	0.056	0.002

Data are expressed as *P* values.

mice (−31%) (data and *P* values of Bonferroni posttests shown in Figure 3, A to C).

Volumes of SM, SL, and SR

Two-way ANOVA indicated significant age-related differences in mean volumes of SM, SL, and SR (see Table 1 for all *P* values). In the case of SM and SR, differences in mean volumes were also significant among the investigated genotypes. However, Bonferroni posttests showed a significant age-related decline only in the mean volume of SM in the $APP751^{SL}/PS1^{M146L}$ mice (on average −26%) (Figure 3, D to F).

SIPB Numbers

As for mean SIPB densities and the mean volumes of SM, SL, and SR, two-way ANOVA indicated significant age-related differences in mean SIPB numbers within all investigated hippocampal subregions (see Table 1 for all *P* values). In the case of SM and SR, differences in mean SIPB numbers were also significant among the investigated genotypes. Bonferroni posttests showed a significant age-related decline in mean SIPB numbers within SM for the wild-type control mice (on average, −19%), the $PS1^{M146L}$ mice (−24%) and the $APP751^{SL}/PS1^{M146L}$ mice (−49%), within SL only for the $APP751^{SL}/PS1^{M146L}$ mice (−33%), and within SR for the $PS1^{M146L}$ mice (−30%) and the $APP751^{SL}/PS1^{M146L}$ mice (−38%) (for data and *P* values of Bonferroni posttests, see Figure 3, G to I).

Corrected SIPB Numbers

Two-way ANOVA revealed statistically significant age- and genotype-related differences in mean corrected SIPB numbers within SM, SL, and SR (the *P* values of two-way ANOVA are given in Table 1). Bonferroni posttests showed a significant age-related decline in mean corrected SIPB numbers within SM for all investigated genotypes (wild-type control mice, −19% on average; $APP751^{SL}$ mice, −19%; $PS1^{M146L}$ mice, −24%; and $APP751^{SL}/PS1^{M146L}$ mice, −56%), within SL only for the $APP751^{SL}/PS1^{M146L}$ mice (−42%) and within SR for all investigated genotypes except for the wild-type control mice ($APP751^{SL}$ mice, −32%; $PS1^{M146L}$ mice, −30%; $APP751^{SL}/PS1^{M146L}$ mice, −51%) (data and *P* values of Bonferroni posttests shown in Figure 3, K to M).

Discussion

Alterations in SIPB Morphology Due to Aβ Deposits

In the present study, enlarged SIPBs were found in the near vicinity of Aβ deposits within the hippocampus of the $APP751^{SL}$ mice and the $APP751^{SL}/PS1^{M146L}$ mice. This finding is in line with several studies in the literature reporting the presence of enlarged SIPBs in AD patients[28] as well as in APP transgenic and APP/PS1 transgenic mice.[21,29–33] Furthermore, dystrophic neurites with swollen varicosities in the near vicinity of Aβ deposits as well as spine loss and shaft atrophy have been reported in APP transgenic and APP/PS1 transgenic mice.[29,30,34,35]

Of particular interest was the observation of a close spatial relationship between aggregated Aβ and enlarged SIPBs in the present study. One may speculate that Aβ deposits are involved in the formation of enlarged SIPBs. In this respect, a study by Phinney et al[36] indicated that Aβ deposits in APP23 mice may attract dystrophic axonal terminals. However, it is also possible that enlarged SIPBs are involved in the production or secretion of Aβ. Recent evidence indicating that axonally transported APP can give rise to Aβ and that Aβ is subsequently released from presynaptic sites and deposited in Aβ deposits *in vivo*[37] may argue for the latter speculation. Furthermore, APP, presenilins, and synaptophysin have been shown to co-localize at the growth cones of developing cultured neurons.[38] In summary, it is reasonable to conclude that Aβ deposits play an important role in degeneration of presynaptic structures and therefore have considerable impact on local synaptic connectivity.

Alterations in SIPB Densities and SIPB Numbers in $APP751^{SL}$ and $APP751^{SL}/PS1^{M146L}$ Transgenic Mice

The wild-type control mice investigated in the present study did not show significant differences in mean SIPB densities within hippocampal subregions SM, SL, and SR and in mean volumes of these subregions between 4.5 months and 17 months of age. Furthermore, an age-related decline in mean SIPB number was only observed within SM but not within SL and SR of the wild-type control mice. These data are in line with previous reports in the literature.[19,20,39,40]

Transgenic expression of human mutant APP and human mutant PS1 in the investigated mice had significant, region-specific effects on mean SIPB densities and SIPB numbers within the investigated hippocampal subregions. Compared with the age-matched wild-type control mice, the $APP751^{SL}$ mice showed transgene-induced

age-related loss of SIPBs only within SR (results of the PS1^{M146L} mice are separately discussed below). Within SM, a similar amount of age-related loss of SIPBs was observed in the wild-type control mice, the APP751^{SL} mice, and the PS1^{M146L} mice. Furthermore, none of these mice showed an age-related loss of SIPBs within SL. In contrast, the APP751^{SL}/PS1^{M146L} mice displayed transgene-induced age-related loss of SIPBs within SM, SL, and SR. Besides this, there was no difference between the wild-type control mice and the APP751^{SL} mice with respect to age-related loss of SIPBs within SR as long as Aβ deposits were not taken into account. In contrast, the APP751^{SL}/PS1^{M146L} mice showed a transgene-induced age-related loss of SIPBs even in regions within SM, SL, and SR free of Aβ deposits (discussed separately below).

Based on the analysis of SIPB densities within the hippocampal subregion SM of APP$_{Wt}$ I63 and APP$_{Ind}$ H6 transgenic mice, Mucke et al[20] suggested evidence for Aβ-induced synaptotoxicity even in the absence of Aβ deposits in APP transgenic mice. This is in contrast to the findings of the present study in which age-related loss of SIPBs in the absence of Aβ deposits was found only for the APP751^{SL}/PS1^{M146L} mice but not for the APP751^{SL} mice. Methodological differences might explain this discrepancy between the findings of Mucke et al[20] and the present study. Mucke et al[20] correlated their SIPB density data with the overall hippocampal plaque load and found no significant correlation between these parameters in their APP transgenic mice. Based on this lack of correlation, these authors concluded that Aβ is synaptotoxic even in the absence of plaques in their APP transgenic mice.[20] However, in the present study, no correlation between SIPB densities within SM and overall hippocampal plaque load was found in the APP751^{SL} mice as well as in the APP751^{SL}/PS1^{M146L} mice (not shown). Rather, correlation analyses between plaque load and other neuropathologic findings in transgenic mouse models of AD may be misleading, as outlined recently.[12] Another reason for the discrepancy between the findings of Mucke et al[20] and the present study might be differences in the transgenic constructs, ie, in the introduced mutations and/or the promoters used. In this regard, it is important to note that the APP transgenic mice investigated by Mucke et al[20] showed a significantly reduced SIPB density within SM compared with wild-type controls already at 2 to 4 months of age. This might reflect a specific neurodevelopmental defect in the APP transgenic mice investigated by these authors. In contrast, in the present study the APP751^{SL} mice had the highest mean SIPB densities as well as (except for SL at M4.5) the highest mean SIPB numbers within SM, SL, and SR among the investigated genotypes at both M4.5 and M17. This might indicate synaptotrophic effects of APP in the APP751^{SL} mice investigated in the present study as known from other transgenic mice expressing different forms of human APP.[41,42] In this regard, it is important to note that Takeuchi et al[33] found slightly higher SIPB densities within hippocampal subregions SM and SR of APP$^{K670N/M671L}$ transgenic mice and of APP$^{K670N/M671L}$/PS1^{M146L} double transgenic mice than within SM and SR of both wild-type control mice and PS1^{M146L} transgenic mice at 12 months of age. These data are fully in line with the results of the present study at M4.5. Wong et al[43] found, compared with wild-type controls, increased densities of vesicular acetylcholine transporter immunoreactive presynaptic boutons within SR of APP$^{KM670/671NL}$ transgenic mice but neither within SR of PS1^{M146L} transgenic mice nor of APP$^{K670N/M671L}$/PS1^{M146L} double transgenic mice at 8 months of age. Except for the results for the APP$^{K670N/M671L}$/PS1^{M146L} double transgenic mice, these data are in line with the findings of the present study at M4.5 as well. Takeuchi et al[33] and Wong et al[43] restricted their analyses to 12-month-old animals (or to 8-month-old animals, respectively). Thus, these studies cannot be compared with the present study with respect to age-related alterations in hippocampal SIPB densities based on transgenic expression of human mutant APP and/or human mutant PS1 in mice. The same holds true for a study by Dodart et al[44] in which SIPB densities within several hippocampal subregions of 12-month-old APP^{V717F} transgenic mice were investigated (on average, no difference between APP^{V717F} transgenic mice and wild-type control mice).

Furthermore, it should be mentioned that King and Arendash[21] observed a decline of approximately 40% in mean SIPB densities within hippocampal subregions SM and SR of wild-type control mice between 3 and 19 months of age and an approximately 40% increase in SIPB densities within SM and SR of APP^{695} transgenic mice. Accordingly, these authors found SIPB densities within SM and SR of 19-month-old APP^{695} transgenic mice approximately twice as high as within SM and SR of 19-month-old wild-type controls.[21] These data are in line neither with the results of the present study nor with the findings of Mucke et al[20] and other reports in the literature concerning age-related alterations in synaptophysin immunoreactivity within the hippocampus of wild-type rodents.[19,20,39,40] Besides differences in the transgenic constructs, the reason for this discrepancy might be due to different methodologies. Seemingly, the image analysis approach of King and Arendash[21] did not focus on the analysis of SIPB densities within regions free of Aβ deposits and Aβ aggregation-related disturbances in normal SIPB morphology. Furthermore, it cannot be excluded that the intense synaptophysin staining demonstrated by King and Arendash[21] for APP^{695} transgenic mice at 19 months of age was affected by intraparenchymal IgG molecules (blocked by using the M.O.M. immunodetection kit (Vector) in the present study).

Finally, Phinney et al[36] observed that Aβ deposits in APP23 mice attracted dystrophic axonal terminals to ectopic locations, which may lead to disruption of normal neuronal connectivity. Accordingly, the intense synaptophysin immunoreactivity at the periphery of neuritic plaques seen in the APP751^{SL} mice and the APP751^{SL}/PS1^{M146L} mice investigated in the present study as well as described in the literature (discussed above) might reflect neurotropic properties of Aβ deposits. One might even ask the question of whether this mechanism could result in reduced SIPB numbers in areas that should have received the projections. The results obtained on the APP751^{SL} mice in the present study may answer this

question. Provided that the main mechanism in SIPB loss in regions free of Aβ deposits would have been the result of inappropriate redirection of projections to cluster around the Aβ deposits (and consequently resulting in deficits in the areas that should have received the projections), the APP751^{SL} mice should have shown significant differences in SIPB densities and numbers (compared with the wild-type control mice) in regions free of Aβ deposits. However, as shown in Figure 3, this was not the case.

In summary, the results of the present study are in line with several reports in the literature, and differences with other reports can be explained. Importantly, to the best of our knowledge, the results of the present study are the first ones demonstrating both quantitative and qualitative differences between the simultaneous transgenic expression of human mutant APP and human mutant PS1 and the single transgenic expression of either human mutant APP or human mutant PS1 in mice on age-related loss of SIPBs within the hippocampus. Potential reasons for these differences are discussed in the next paragraphs.

Alterations in SIPB Densities and SIPB Numbers in PS1^{M146L} Transgenic Mice

Of particular importance was the finding of a transgene-induced age-related reduction in both mean SIPB density and mean SIPB number within the hippocampal subregion SR (CA1–2) of the PS1^{M146L} mice in the present study. To the best of our knowledge, these are the first results demonstrating a region-specific effect of transgenic expression of human mutant PS1 on age-related loss of SIPBs within the mouse hippocampus.

Presenilins are considered to be the catalytic subunits of the γ-secretase complex, but they are also essential for the fine tuning of the immunological system and for memory and synaptic plasticity.[45] AD-associated presenilin mutations clearly affect γ-secretase cleavage and thereby enhance Aβ generation.[10] According to previous observations by Duff et al,[46] expression of mutant PS1 itself may generate murine Aβ. We have previously investigated the presence of human Aβ in the PS1^{M146L} mice and found no Aβ signal in ELISA blots using a monoclonal antibody (WO-2) against human Aβ.[10] However, we cannot exclude that there was at least some generation of endogenous murine Aβ (possibly not detectable by the antibody used in our previous study) in the PS1^{M146L} mice. On the other hand, we detected considerable amounts of Aβ in the APP751^{SL} mice.[10] The fact that we found more age-related SIPB loss within SM and SR of the PS1^{M146L} mice than within SM and SR of the APP751^{SL} mice would argue that other factors rather than Aβ were the driving force in SIPB loss in the PS1^{M146L} mice. In this respect, it is important to address that presenilins affect intracellular calcium stores, protein trafficking and protein turnover, and neuronal signaling.[47] Consequently, it has been proposed that destabilization of calcium signaling has a role in neurodegeneration in AD.[47] Mutations in PS1 and PS2 are known to perturb endoplasmic reticulum calcium homeostasis such that greater amounts of calcium are released on stimulation.[48,49] Furthermore, Herms et al[50] showed deregulation of intracellular calcium homeostasis by decreased capacitative calcium entry in hippocampal neurons dissociated from newborn mice transgenic for mutant PS1^{A246E} (capacitative calcium entry being a refill mechanism allowing entry of extracellular calcium ions through plasma membrane channels that are tightly regulated by and even physically linked to intracellular stores[51]). Importantly, calcium-induced formation of reactive oxidative species and mitochondrial swelling were found to be higher in isolated rat mitochondria from the CA1 than from the CA3 region.[52] Furthermore, synaptosomal proteins from PS1^{M146V} knock-in mice displayed increased oxidative stress compared with synaptosomal proteins from wild-type mice.[53] Begley et al[54] observed evidence of disturbed calcium homeostasis and mitochondrial dysfunction in synaptosomes prepared from mice transgenic for mutant PS1; it is reasonable to hypothesize that similar to the knock-in mice studied by LaFontaine et al,[53] synaptosomal proteins were also affected by increased oxidative stress in the transgenic mice investigated by Begley et al.[54] Moreover, it was recently shown that expression of the PS1 mutations M146V, I143T, and deletion of exon 9 in human neuronal cells *in vitro* significantly increased the activation of glycogen synthase kinase 3-β (GSK3-β).[55] *In vivo*, GSK3-β phosphorylates kinesin light chains and causes the release of kinesin-I from membrane-bound organelles, leading to a reduction in kinesin-I-mediated fast axonal transport.[56] Consistent with such a deficit in kinesin-I-mediated fast axonal transport, densities of synaptophysin-containing vesicles and mitochondria were found reduced in neuritic processes of hippocampal neurons expressing mutant PS1^{M146V} *in vitro*.[55] On the basis of these findings, it is attractive to speculate that the observed transgene-induced age-related loss of SIPBs within SR of the PS1^{M146L} mice in the present study was connected to transgene-induced alterations in cellular calcium homeostasis, fast axonal transport, and the formation of reactive oxidative species. At least the latter mechanism might occur preferentially within the hippocampal CA1 region, therefore triggering age-related SIPB loss preferentially within SR. Interestingly, perturbations in calcium homeostasis and alterations in GSK3-β activation caused by mutations in PS1 might be connected to each other. Calcium signaling activates the phosphatase calcineurin and induces movement of NFATc proteins into the nucleus, whereas nuclear import of NFATc proteins is opposed by kinases such as GSK3-β.[57]

Besides these mechanisms, recent studies indicated that presenilins also mediate cleavage of synaptic-associated adhesion molecules such as nectin1α[58] and cadherins.[59] However, it remains to be determined whether PS1 cadherin/catenin interaction or PS-mediated cleavage of adhesion molecules play a functional role in synapse formation or modulate synaptic activity.[60] Thus, one can only speculate whether altered PS1-mediated cleavage of synaptic-associated adhesion proteins influenced synaptic function and integrity and was involved in the

reported age-related loss of SIPBs within SR of the PS1^{M146L} mice.

Finally, it should be mentioned that in a recent study on 3-month-old mice in which the M146V mutation of PS1 was knocked in into the endogenous mouse PS1 gene, Wang et al[61] found impaired hippocampus-dependent contextual learning and reduced adult neurogenesis in the dentate gyrus. The latter result is in line with earlier findings of increased cell cycle arrest caused by PS1 mutations overexpressed in cells *in vitro*.[62] On the other hand, total numbers of hippocampal granule cells were found unchanged compared with wild-type controls in mice transgenic for the same PS1 mutation as investigated by Wang et al[61] as well as in mice in which the human PS1 mutations M233T and L235P were knocked in into the mouse PS1 gene.[12,63] Thus, the possible impact of reduced neurogenesis in the dentate gyrus of PS1^{M146V} knock-in mice on hippocampus-dependent contextual learning remains elusive.

In summary, the finding of a transgene-induced age-related loss of SIPBs within the hippocampal subregion SR of the PS1^{M146L} mice in the present study can be explained by potential mechanisms of mutant PS1 reported in the literature. One can regard the findings of the present study as among the first *in vivo* evidence for a role of mutant PS1 in neurodegeneration without concomitant neuron loss, apart from its contribution to alterations in Aβ generation. This might serve as the basis for further modifying the amyloid hypothesis of neurodegeneration in AD.[14]

Alterations in SIPB Densities and SIPB Numbers in APP751^{SL}/PS1^{M146L} Transgenic Mice Independent of Aβ Deposits

As explained above, there was no difference between the wild-type control mice and the APP751^{SL} mice with respect to age-related loss of SIPBs as long as Aβ deposits were not taken into account. It can therefore not be excluded that local development of Aβ deposits fully accounted for the loss of SIPBs seen within hippocampal subregion SR of the APP751^{SL} mice at M17. In contrast, the APP751^{SL}/PS1^{M146L} mice showed a transgene-induced age-related loss of SIPBs even in regions within SM, SL, and SR free of Aβ deposits. This phenomenon can be due to several interacting mechanisms: 1) The aforementioned potential actions of mutant PS1 (at least within SR). 2) Local neuron loss. Our previous study on the same APP751^{SL}/PS1^{M146L} mice showed a substantial age-related loss of hippocampal pyramidal cells (on average approximately 30%).[12] Loss of hippocampal pyramidal cells resulted most probably in a decreased number of dendrites in SL and SR. Thus, one cannot exclude that the combined action of hippocampal pyramidal cell loss and Aβ deposits within SL and SR fully accounted for the loss of SIPBs seen within these regions of the APP751^{SL}/PS1^{M146L} mice. At M17, these mice showed a transgene-induced age-related reduction in mean SIPB numbers of 33% in regions within SL (and of 38% in regions within SR, respectively) free of Aβ deposits and an approximately 30% loss of pyramidal cells within the hippocampus.[12] 3) Neuron loss in regions with heavy projections to the areas analyzed. In this regard, we have previously shown that age-related neuron loss occurred within the hippocampal pyramidal cell layer but not within the hippocampal granule cell layer of the APP751^{SL}/PS1^{M146L} mice,[12] ie, exactly the same mice as investigated in the present study. The mossy fibers (ie, the axons of the hippocampal granule cells) project to the hippocampal pyramidal cells (mainly to CA3). Thus, the effects seen in the SL of the APP751^{SL}/PS1^{M146L} mice cannot be explained by neuron loss in the region projecting to SL. Furthermore, age-related loss of SIPBs was found in SR of the PS1^{M146L} mice, which did not show age-related neuron loss in any hippocampal area.[12] Preliminary evidence from microscopic inspection suggested age-related neuron loss in the entorhinal cortex of the APP^{751SL}/PS1^{M146L} mice but not in the PS1^{M146L} mice (not shown) that showed SIPB loss within SM. Together, these data indicate that loss of neurons at regions with heavy projections toward the areas analyzed in the present study was of limited impact on age-related SIPB loss. 4) Action of soluble Aβ. Soluble Aβ species have been demonstrated to induce neurotoxicity, which is likely to provoke neuropathology reminiscent of AD[64,65] (see also Refs. [2] and [66–68]). In this regard, a 12% reduction in total dendritic length of hippocampal granule cells was found in 3-month-old APP^{V717F} transgenic mice, ie, before amyloid deposition, in a recent study by Wu et al.[69] Certain subsets of granule cells (superficially located granule cells in the dorsal blade of the dentate gyrus) even exhibited a 23% loss of total dendritic length at 3 months of age.[69] The authors of this study hypothesized that these alterations were due to elevated levels of soluble forms of Aβ, induced by the overexpression of APP.[69] Comparably, one may speculate that at least part of the 30% (49% minus 19% age-related loss of SIPB numbers seen within SM of the wild-type control mice) transgene-induced age-related reduction in SIPB numbers in regions free of Aβ deposits within SM of APP751^{SL}/PS1^{M146L} mice is due to elevated levels of soluble Aβ. 5) Intraneuronal Aβ. Previous reports have shown that intraneuronal Aβ preceded the formation of Aβ deposits in APP751^{SL}/PS1^{M146L} mice[9] and that elevated levels of intraneuronal Aβ were associated with several alterations in normal cell homeostasis.[11,14,64,70] Moreover, intraneuronal Aβ has been reported to substantially affect synaptic function[26] and integrity.[71] 6) A chronic inflammation status. Previously, we reported widespread microglia activation within the hippocampal neuropil of APP751^{SL}/PS1^{M146L} mice that was only partly related to Aβ deposits.[12] Thus, one could argue that microglia activation might be an early pathogenic event preceding loss of SIPBs and possibly having a causative role in SIPB loss.[72,73]

With respect to the potential impact of both soluble forms of Aβ and intraneuronal Aβ on SIPB loss in hippocampal regions free of Aβ deposits, analysis of SIPB densities and numbers in the hippocampus of APP^{SL}/PS1KI mice[70] will be important. This is due to the fact that mutations in PS1 have been shown to enhance γ-secretase activity toward elevated Aβ42 generation.[74–76] The Aβ42/Aβ ratio was approximately 0.2 in the APP751^{SL} mice and approximately 0.4 in the APP751^{SL}/PS1^{M146L} mice investigated here[11] and was increased to approximately 0.85 in APP^{SL}/PS1KI mice that showed profound

hippocampal neuron loss and intraneuronal accumulation of Aβ already at 10 months of age.[70] We hypothesize that in the hippocampus of APP^{SL}/PS1KI mice, profound SIPB loss will also be found in regions free of Aβ deposits, and the comparison of results from APP751^{SL}/PS1^{M146L} mice and APP^{SL}/PS1KI mice will provide novel insights into the impact of transgenic expression and "knock-in" expression of mutations of PS1 on impairments of synaptic integrity in AD.

Relevance of the Findings of the Present Study to Human AD

Loss of hippocampal synaptophysin immunoreactivity was established as an early marker in human AD but did not show spatial correlation with Aβ deposits.[77] By simultaneously investigating the formation of neurofibrillary tangles and the relative amount of synaptophysin mRNA within the same neurons, a number of studies indicated evidence for a tangle-dependent mechanism of hippocampal synaptophysin loss in AD.[78–80] However, the formation of tangles accounts for only a small proportion of loss of hippocampal neurons in AD, at least within area CA1.[81] Accordingly, the formation of tangles is most probably not the predominant mechanism of hippocampal synaptophysin loss in AD. This is supported by the finding of no local correlation between the degree of synaptophysin-like immunoreactivity and CD-1 immunoreactive neurons within the hippocampus of brains from patients with AD (with the CD-1 antibody recognizing tangles, dystrophic neurites in and around Aβ deposits, and neuropil threads).[77] Rather, Callahan et al[80] recently found that hippocampal CA1 neurons free of both tangles and immunohistochemical detectable tau phosphorylation at Ser 262, 356 and 396/404 in brains from patients with AD (Braak stage V-VI[82]) showed a statistically significant reduction of more than 20% in the relative amount of synaptophysin mRNA compared with corresponding neurons in brains from controls (Braak stage I-II).

These data indicate that hippocampal synaptophysin loss in AD seems to be multifactorial. In this regard, the simultaneous analysis of the APP751^{SL} mice, the PS1^{M146L} mice, and the APP751^{SL}/PS1^{M146L} mice investigated in the present study offers a unique framework to test hypotheses on the impact of several molecular and cellular events caused by transgenic expression of human mutant APP and/or human mutant PS1 on age-related alterations in synaptic integrity. First, the transgene-induced age-related SIPB loss seen within hippocampal subregion SR of the APP751^{SL} mice might be almost completely due to Aβ deposits. This hypothesis can be tested by vaccination or other approaches focusing on the prevention of Aβ aggregation. Second, the transgene-induced age-related SIPB loss seen within SL and SR of the APP751^{SL}/PS1^{M146L} mice might be almost completely due to the combined action of Aβ deposits and neuron loss. This offers for the first time the possibility to address the question of whether alterations in synaptic integrity precede neuron loss in a transgenic animal model of AD. Third, the transgene-induced age-related SIPB loss seen within SR of the PS1^{M146L} mice cannot be attributed to Aβ deposits or to neuron loss. This offers, for the first time, the possibility to study actions of mutant PS1 in neurodegeneration apart from its contribution to altered APP processing and Aβ generation. Finally, the transgene-induced age-related SIPB loss seen within SM of the APP751^{SL}/PS1^{M146L} mice can also neither be attributed to Aβ deposits nor to neuron loss. As age-related SIPB loss within SM of the PS1^{M146L} mice did not exceed age-related SIPB loss within this hippocampal subregion of the wild-type control mice, one might speculate that the age-related SIPB loss within SM of the APP751^{SL}/PS1^{M146L} mice that could not be explained by Aβ deposits and neuron loss was not due to actions of mutant PS1. Thus SIPB loss in APP751^{SL}/PS1^{M146L} is most probably due to complex interactions between the Aβ deposits, neuronal loss locally or at a distance, generation of intraneuronal and soluble Aβ, and other PS1 mediated actions.

In summary, the transgenic mouse models as investigated in our study can be seen among the best animal models of AD and provide, for the first time, the possibility to investigate hippocampal subregion-specific differences in interactions between neuron loss, Aβ deposits, soluble Aβ, intraneuronal Aβ, and PS1-mediated actions on alterations in synaptic integrity. Future experiments are likely to have further significant impact on the field of AD research.

Acknowledgments

We thank V. Blanchard-Bregeon and L. Pradier for providing the transgenic animals and E. Barth, H. Helten, D. Van Iersel, W. Engels, and H.P.J. Steinbusch for their excellent assistance.

References

1. Cummings JL: Alzheimer's disease. N Engl J Med 2004, 351:56–67
2. Selkoe DJ: Alzheimer's disease is a synaptic failure. Science 2002, 298:789–791
3. Morrison JH, Hof PR: Selective vulnerability of corticocortical and hippocampal circuits in aging and Alzheimer's disease. Prog Brain Res 2002, 136:467–486
4. Hardy J, Selkoe DJ: The amyloid hypothesis of Alzheimer's disease: progress and problems on the road to therapeutics. Science 2002, 297:353–356
5. Scheff SW, Price DA: Synaptic pathology in Alzheimer's disease: a review of ultrastructural studies. Neurobiol Aging 2003, 24:1029–1046
6. Small DH, Mok SS, Bornstein JC: Alzheimer's disease and Abeta toxicity: from top to bottom. Nat Rev Neurosci 2001, 2:595–598
7. Davies CA, Mann DM, Sumpter PQ, Yates PO: A quantitative morphometric analysis of the neuronal and synaptic content of the frontal and temporal cortex in patients with Alzheimer's disease. J Neurol Sci 1987, 78:151–164
8. Hof PR, Morrison JH: The aging brain: morphomolecular senescence of cortical circuits. Trends Neurosci 2004, 27:607–613
9. Wirths O, Multhaup G, Czech C, Blanchard V, Moussaoui S, Tremp G, Pradier L, Beyreuther K, Bayer TA: Intraneuronal Abeta accumulation precedes plaque formation in beta-amyloid precursor protein and presenilin-1 double-transgenic mice. Neurosci Lett 2001, 306:116–120
10. Wirths O, Multhaup G, Czech C, Feldmann N, Blanchard V, Tremp G, Beyreuther K, Pradier L, Bayer TA: Intraneuronal APP/A beta traffick-

ing and plaque formation in beta-amyloid precursor protein and presenilin-1 transgenic mice. Brain Pathol 2002, 12:275–286
11. Blanchard V, Moussaoui S, Czech C, Touchet N, Bonici B, Planche M, Canton T, Jedidi I, Gohin M, Wirths O, Bayer TA, Langui D, Duyckaerts C, Tremp G, Pradier L: Time sequence of maturation of dystrophic neurites associated with Abeta deposits in APP/PS1 transgenic mice. Exp Neurol 2003, 184:247–263
12. Schmitz C, Rutten BP, Pielen A, Schafer S, Wirths O, Tremp G, Czech C, Blanchard V, Multhaup G, Rezaie P, Korr H, Steinbusch HW, Pradier L, Bayer TA: Hippocampal neuron loss exceeds amyloid plaque load in a transgenic mouse model of Alzheimer's disease. Am J Pathol 2004, 164:1495–1502
13. Dickson DW: Building a more perfect beast: aPP transgenic mice with neuronal loss. Am J Pathol 2004, 164:1143–1146
14. Wirths O, Multhaup G, Bayer TA: A modified beta-amyloid hypothesis: intraneuronal accumulation of the beta-amyloid peptide—the first step of a fatal cascade. J Neurochem 2004, 91:513–520
15. Van de Berg WDJ, Blokland A, Schmitz C, Cuello AC, Steinbusch HWM, Blanco CE: Synaptic numbers in striatum and cortex of aged rats following perinatal asphyxia: a stereologic and behavioral correlative analysis. J Chem Neuroanat 2000, 20:71–82
16. Rutten BP, Wirths O, Van de Berg WD, Lichtenthaler SF, Vehoff J, Steinbusch HW, Korr H, Beyreuther K, Multhaup G, Bayer TA, Schmitz C: No alterations of hippocampal neuronal number and synaptic bouton number in a transgenic mouse model expressing the beta-cleaved C-terminal APP fragment. Neurobiol Dis 2003, 12:110–120
17. Masliah E, Terry RD, DeTeresa RM, Hansen LA: Immunohistochemical quantification of the synapse-related protein synaptophysin in Alzheimer disease. Neurosci Lett 1989, 103:234–239
18. Wong TP, Campbell PM, Ribeiro-da-Silva A, Cuello AC: Synaptic numbers across cortical laminae and cognitive performance of the rat during ageing. Neuroscience 1998, 84:403–412
19. Smith TD, Adams MM, Gallagher M, Morrison JH, Rapp PR: Circuit-specific alterations in hippocampal synaptophysin immunoreactivity predict spatial learning impairment in aged rats. J Neurosci 2000, 20:6587–6593
20. Mucke L, Masliah E, Yu GQ, Mallory M, Rockenstein EM, Tatsuno G, Hu K, Kholodenko D, Johnson-Wood K, McConlogue L: High-level neuronal expression of abeta 1–42 in wild-type human amyloid protein precursor transgenic mice: synaptotoxicity without plaque formation. J Neurosci 2000, 20:4050–4058
21. King DL, Arendash GW: Maintained synaptophysin immunoreactivity in Tg2576 transgenic mice during aging: correlations with cognitive impairment. Brain Res 2002, 926:58–68
22. Borchardt T, Camakaris J, Cappai R, Masters CL, Beyreuther K, Multhaup G: Copper inhibits beta-amyloid production and stimulates the non-amyloidogenic pathway of amyloid-precursor-protein secretion. Biochem J 1999, 344:461–467
23. van Zandvoort M, Engels W, Douma K, Beckers L, Oude Egbrink M, Daemen M, Slaaf DW: Two-photon microscopy for imaging of the (atherosclerotic) vascular wall: a proof of concept study. J Vasc Res 2004, 41:54–63
24. Franklin KBJ, Paxinos G: The Mouse Brain in Stereotaxic Coordinates. San Diego, Academic Press, 1996
25. Gundersen HJ, Jensen EB: The efficiency of systematic sampling in stereology and its prediction. J Microsc 1987, 147:229–263
26. Schmitz C, Hof PR: Design-based stereology in neuroscience. Neuroscience 2004, 130:813–831
27. Miles RE, Davy PJ: Precise and general conditions for the validity of a comprehensive set of stereological fundamental formulae. J Microsc 1976, 107:211–226
28. Bugiani O, Giaccone G, Verga L, Pollo B, Ghetti B, Frangione B, Tagliavini F: Alzheimer patients and Down patients: abnormal presynaptic terminals are related to cerebral preamyloid deposits. Neurosci Lett 1990, 119:56–59
29. Tsai J, Grutzendler J, Duff K, Gan WB: Fibrillar amyloid deposition leads to local synaptic abnormalities and breakage of neuronal branches. Nat Neurosci 2004, 7:1181–1183
30. Delatour B, Blanchard V, Pradier L, Duyckaerts C: Alzheimer pathology disorganizes cortico-cortical circuitry: direct evidence from a transgenic animal model. Neurobiol Dis 2004, 16:41–47
31. Brendza RP, O'Brien C, Simmons K, McKeel DW, Bales KR, Paul SM, Olney JW, Sanes JR, Holtzman DM: PDAPP; YFP double transgenic mice: a tool to study amyloid-beta associated changes in axonal, dendritic, and synaptic structures. J Comp Neurol 2003, 456:375–383
32. Rockenstein E, Mallory M, Mante M, Sisk A, Masliaha E: Early formation of mature amyloid-beta protein deposits in a mutant APP transgenic model depends on levels of Abeta(1–42). J Neurosci Res 2001, 66:573–582
33. Takeuchi A, Irizarry MC, Duff K, Saido TC, Hsiao Ashe K, Hasegawa M, Mann DM, Hyman BT, Iwatsubo T: Age-related amyloid beta deposition in transgenic mice overexpressing both Alzheimer mutant presenilin 1 and amyloid beta precursor protein Swedish mutant is not associated with global neuronal loss. Am J Pathol 2000, 157:331–339
34. Sturchler-Pierrat C, Abramowski D, Duke M, Wiederhold KH, Mistl C, Rothacher S, Ledermann B, Burki K, Frey P, Paganetti PA, Waridel C, Calhoun ME, Jucker M, Probst A, Staufenbiel M, Sommer B: Two amyloid precursor protein transgenic mouse models with Alzheimer disease-like pathology. Proc Natl Acad Sci USA 1997, 94:13287–13292
35. Boutajangout A, Authelet M, Blanchard V, Touchet N, Tremp G, Pradier L, Brion JP: Characterisation of cytoskeletal abnormalities in mice transgenic for wild-type human tau and familial Alzheimer's disease mutants of APP and presenilin-1. Neurobiol Dis 2004, 15:47–60
36. Phinney AL, Deller T, Stalder M, Calhoun ME, Frotscher M, Sommer B, Staufenbiel M, Jucker M: Cerebral amyloid induces aberrant axonal sprouting and ectopic terminal formation in amyloid precursor protein transgenic mice. J Neurosci 1999, 19:8552–8559
37. Lazarov O, Lee M, Peterson DA, Sisodia SS: Evidence that synaptically released beta-amyloid accumulates as extracellular deposits in the hippocampus of transgenic mice. J Neurosci 2002, 22:9785–9793
38. Ribaut-Barassin C, Dupont JL, Haeberle AM, Bombarde G, Huber G, Moussaoui S, Mariani J, Bailly Y: Alzheimer's disease proteins in cerebellar and hippocampal synapses during postnatal development and aging of the rat. Neuroscience 2003, 120:405–423
39. Nicolle MM, Gallagher M, McKinney M: No loss of synaptic proteins in the hippocampus of aged, behaviorally impaired rats. Neurobiol Aging 1999, 20:343–348
40. Calhoun ME, Kurth D, Phinney AL, Long JM, Hengemihle J, Mouton PR, Ingram DK, Jucker M: Hippocampal neuron and synaptophysin-positive bouton number in aging C57BL/6 mice. Neurobiol Aging 1998, 19:599–606
41. Mucke L, Abraham CR, Masliah E: Neurotrophic and neuroprotective effects of hAPP in transgenic mice. Ann NY Acad Sci 1996, 777:82–88
42. Mucke L, Masliah E, Johnson WB, Ruppe MD, Alford M, Rockenstein EM, Forss-Petter S, Pietropaolo M, Mallory M, Abraham CR: Synaptotrophic effects of human amyloid beta protein precursors in the cortex of transgenic mice. Brain Res 1994, 666:151–167
43. Wong TP, Debeir T, Duff K, Cuello AC: Reorganization of cholinergic terminals in the cerebral cortex and hippocampus in transgenic mice carrying mutated presenilin-1 and amyloid precursor protein transgenes. J Neurosci 1999, 19:2706–2716
44. Dodart JC, Mathis C, Saura J, Bales KR, Paul SM, Ungerer A: Neuroanatomical abnormalities in behaviorally characterized APP(V717F) transgenic mice. Neurobiol Dis 2000, 7:71–85
45. Marjaux E, Hartmann D, De Strooper B: Presenilins in memory, Alzheimer's disease, and therapy. Neuron 2004, 42:189–192
46. Duff K, Eckman C, Zehr C, Yu X, Prada CM, Perez-tur J, Hutton M, Buee L, Harigaya Y, Yager D, Morgan D, Gordon MN, Holcomb L, Refolo L, Zenk B, Hardy J, Younkin S: Increased amyloid-beta42(43) in brains of mice expressing mutant presenilin 1. Nature 1996, 383:710–713
47. Koo EH, Kopan R: Potential role of presenilin-regulated signaling pathways in sporadic neurodegeneration. Nat Med 2004, 10:S26–S33
48. Chan SL, Furukawa K, Mattson MP: Presenilins and APP in neuritic and synaptic plasticity: implications for the pathogenesis of Alzheimer's disease. Neuromolecular Med 2002, 2:167–196
49. Mattson MP, Chan SL: Neuronal and glial calcium signaling in Alzheimer's disease. Cell Calcium 2003, 34:385–397
50. Herms J, Schneider I, Dewachter I, Caluwaerts N, Kretzschmar H, Van Leuven F: Capacitive calcium entry is directly attenuated by mutant presenilin-1, independent of the expression of the amyloid precursor protein. J Biol Chem 2003, 278:2484–2489
51. Blaustein MP, Golovina VA: Structural complexity and functional di-

versity of endoplasmic reticulum Ca(2+) stores. Trends Neurosci 2001, 24:602–608
52. Mattiasson G, Friberg H, Hansson M, Elmer E, Wieloch T: Flow cytometric analysis of mitochondria from CA1 and CA3 regions of rat hippocampus reveals differences in permeability transition pore activation. J Neurochem 2003, 87:532–544
53. LaFontaine MA, Mattson MP, Butterfield DA: Oxidative stress in synaptosomal proteins from mutant presenilin-1 knock-in mice: implications for familial Alzheimer's disease. Neurochem Res 2002, 27:417–421
54. Begley JG, Duan W, Chan S, Duff K, Mattson MP: Altered calcium homeostasis and mitochondrial dysfunction in cortical synaptic compartments of presenilin-1 mutant mice. J Neurochem 1999, 72:1030–1039
55. Pigino G, Morfini G, Pelsman A, Mattson MP, Brady ST, Busciglio J: Alzheimer's presenilin 1 mutations impair kinesin-based axonal transport. J Neurosci 2003, 23:4499–4508
56. Morfini G, Szebenyi G, Elluru R, Ratner N, Brady ST: Glycogen synthase kinase-3 phosphorylates kinesin light chains and negatively regulates kinesin-based motility. EMBO J 2002, 21:281–293
57. Crabtree GR, Olson EN: NFAT signaling: choreographing the social lives of cells. Cell 2002, 109:S67–S79
58. Kim DY, Ingano LA, Kovacs DM: Nectin-1alpha, an immunoglobulin-like receptor involved in the formation of synapses, is a substrate for presenilin/gamma-secretase-like cleavage. J Biol Chem 2002, 277:49976–49981
59. Georgakopoulos A, Marambaud P, Efthimiopoulos S, Shioi J, Cui W, Li HC, Schutte M, Gordon R, Holstein GR, Martinelli G, Mehta P, Friedrich VL Jr, Robakis NK: Presenilin-1 forms complexes with the cadherin/catenin cell-cell adhesion system and is recruited to intercellular and synaptic contacts. Mol Cell 1999, 4:893–902
60. Thinakaran G, Parent AT: Identification of the role of presenilins beyond Alzheimer's disease. Pharmacol Res 2004, 50:411–418
61. Wang R, Dineley KT, Sweatt JD, Zheng H: Presenilin 1 familial Alzheimer's disease mutation leads to defective associative learning and impaired adult neurogenesis. Neuroscience 2004, 126:305–312
62. Janicki SM, Stabler SM, Monteiro MJ: Familial Alzheimer's disease presenilin-1 mutants potentiate cell cycle arrest. Neurobiol Aging 2000, 21:829–836
63. Van der Kolk N, van de Steeg E, Rutten BPF, Wirths O, Blanchard V, Itier J, Tremp G, Steinbusch HWM, Pradier L, Bayer TA, Schmitz C: Age-related early hippocampal neuron loss in a novel transgenic/knock-in mouse model of AD. Soc Neurosci Abstr 2004, 338:4
64. Oddo S, Caccamo A, Shepherd JD, Murphy MP, Golde TE, Kayed R, Metherate R, Mattson MP, Akbari Y, LaFerla FM: Triple-transgenic model of Alzheimer's disease with plaques and tangles: intracellular Abeta and synaptic dysfunction. Neuron 2003, 39:409–421
65. Lue LF, Kuo YM, Roher AE, Brachova L, Shen Y, Sue L, Beach T, Kurth JH, Rydel RE, Rogers J: Soluble amyloid beta peptide concentration as a predictor of synaptic change in Alzheimer's disease. Am J Pathol 1999, 155:853–862
66. Walsh DM, Selkoe DJ: Deciphering the molecular basis of memory failure in Alzheimer's disease. Neuron 2004, 44:181–193
67. Rowan MJ, Klyubin I, Cullen WK, Anwyl R: Synaptic plasticity in animal models of early Alzheimer's disease. Philos Trans R Soc Lond B Biol Sci 2003, 358:821–828
68. Klein WL, Krafft GA, Finch CE: Targeting small Abeta oligomers: the solution to an Alzheimer's disease conundrum? Trends Neurosci 2001, 24:219–224
69. Wu CC, Chawla F, Games D, Rydel RE, Freedman S, Schenk D, Young WG, Morrison JH, Bloom FE: Selective vulnerability of dentate granule cells prior to amyloid deposition in PDAPP mice: digital morphometric analyses. Proc Natl Acad Sci USA 2004, 101:7141–7146
70. Casas C, Sergeant N, Itier JM, Blanchard V, Wirths O, van der Kolk N, Vingtdeux V, van de Steeg E, Ret G, Canton T, Drobecq H, Clark A, Bonici B, Delacourte A, Benavides J, Schmitz C, Tremp G, Bayer TA, Benoit P, Pradier L: Massive CA1/2 neuronal loss with intraneuronal and N-terminal truncated Abeta42 accumulation in a novel Alzheimer transgenic model. Am J Pathol 2004, 165:1289–1300
71. Takahashi RH, Almeida CG, Kearney PF, Yu F, Lin MT, Milner TA, Gouras GK: Oligomerization of Alzheimer's beta-amyloid within processes and synapses of cultured neurons and brain. J Neurosci 2004, 24:3592–3599
72. Arends YM, Duyckaerts C, Rozemuller JM, Eikelenboom P, Hauw JJ: Microglia, amyloid and dementia in Alzheimer's disease: a correlative study. Neurobiol Aging 2000, 21:39–47
73. Cagnin A, Brooks DJ, Kennedy AM, Gunn RN, Myers R, Turkheimer FE, Jones T, Banati RB: In-vivo measurement of microglia in dementia. Lancet 2000, 358:461–467
74. Borchelt DR, Thinakaran G, Eckman CB, Lee MK, Davenport F, Ratovitsky T, Prada CM, Kim G, Seekins S, Yager D, Slunt HH, Wang R, Seeger M, Levey AI, Gandy SE, Copeland NG, Jenkins NA, Price DL, Younkin SG, Sisodia SS: Familial Alzheimer's disease-linked presenilin 1 variants elevate Abeta1–42/1–40 ratio in vitro and in vivo. Neuron 1996, 17:1005–1013
75. Xia W, Zhang J, Kholodenko D, Citron M, Podlisny MB, Teplow DB, Haass C, Seubert P, Koo EH, Selkoe DJ: Enhanced production and oligomerization of the 42-residue amyloid beta-protein by Chinese hamster ovary cells stably expressing mutant presenilins. J Biol Chem 1997, 272:7977–7982
76. Sisodia SS, St George-Hyslop PH: gamma-Secretase, Notch, Abeta and Alzheimer's disease: where do the presenilins fit in? Nat Rev Neurosci 2002, 3:281–290
77. Heinonen O, Soininen H, Sorvari H, Kosunen O, Paljarvi L, Koivisto E, Riekkinen PJ Sr: Loss of synaptophysin-like immunoreactivity in the hippocampal formation is an early phenomenon in Alzheimer's disease. Neuroscience 1995, 64:375–384
78. Callahan LM, Coleman PD: Neurons bearing neurofibrillary tangles are responsible for selected synaptic deficits in Alzheimer's disease. Neurobiol Aging 1995, 16:311–314
79. Callahan LM, Vaules WA, Coleman PD: Quantitative decrease in synaptophysin message expression and increase in cathepsin D message expression in Alzheimer disease neurons containing neurofibrillary tangles. J Neuropathol Exp Neurol 1999, 58:275–287
80. Callahan LM, Vaules WA, Coleman PD: Progressive reduction of synaptophysin message in single neurons in Alzheimer disease. J Neuropathol Exp Neurol 2002, 61:384–395
81. Kril JJ, Patel S, Harding AJ, Halliday GM: Neuron loss from the hippocampus of Alzheimer's disease exceeds extracellular neurofibrillary tangle formation. Acta Neuropathol 2002, 103:370–376
82. Braak H, Braak E: Neuropathological staging of Alzheimer-related changes. Acta Neuropathol 1991, 82:239–259